low level ($\alpha = 0.1$). However, when the shear stress keeps increasing, K_σ deviates significantly. For loose sand, at $\alpha = 0.4$, K_σ approaches to zero at $\sigma_{nc}' = 500$ kPa. It represents a state of high contractiveness. For even looser sand, as indicated by the test results on Toyoura sand at D_{rc} = 10% (not shown here), a shear stress level of $\alpha = 0.1$ is sufficiently high to deviate the K_σ curve from the general trend. For medium dense sand, the K_σ trends remain similar regardless of the α levels (up to $\alpha = 0.4$). Apparently, the dependence of K_σ on α is state-dependent.

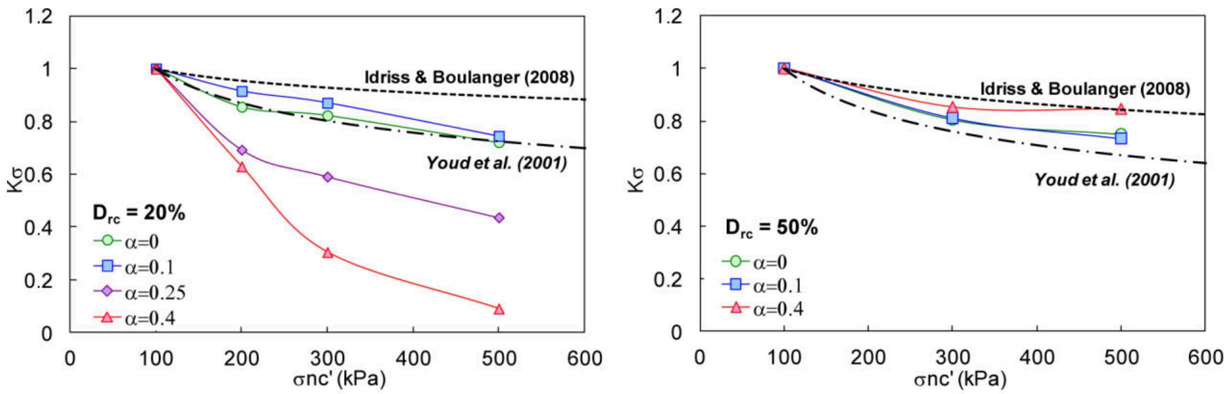

(a) (b)

Figure 6. Plots of K_σ against σ_{nc}' at different α levels for: (a) loose sand at D_{rc} = 20%; (b) medium dense sand at D_{rc} = 50%.

Plotted alongside with the curves in Figure 6 are the K_σ predictions using the correlations proposed by Youd et al. (2001) and Idriss & Boulanger (2008) respectively. Either correlation predicts the K_σ trends pretty well especially for medium dense sand, which is rather immune to the effect of initial sustained shear, but not for loose sand. As discussed previously, both correlations consider K_σ as a function of relative density and effective confining pressure only. They cannot capture the α effect on K_σ especially for sand at a contractive state. In practice, it may result in an over-estimation of the liquefaction resistance extrapolated using the present K_σ correlations. Such over-estimation becomes more prominent in contractive soil, where the results of liquefaction failure are often more disastrous.

Review of K_σ Data from the Literature

Literature data concerning the effects of initial sustained shear on K_σ remains scarce. Some relevant data representative of other testing conditions was collected, and critically reviewed. For example, Hyodo et al. (2002) examined the cyclic triaxial shear behaviour of a Japanese sand. Saturated dense specimen was tested under a wide range of confining pressures up to 5 MPa applied in both isotropic and anisotropic conditions. Their results are re-interpreted in the context of this study, as shown in Figure 7(a). Figure 7(b) shows a batch of cyclic simple shear test data obtained from Sivathayalan & Ha (2004). They tested dry silica sand prepared at a dense state under different confining and static shear stress levels. In both cases, the α effects on K_σ are evident. The results are consistent with the findings of this study.

It is further noted that the α effect is remarkable even the sand specimens were prepared to a dense state. One possible reason is the application of very high confining pressure (see Figure 7(a)), under which the soil tends to exhibit more contractive behaviour. Another possible reason is probably the use of air pluviation method for sample reconstitution in both studies. According to Sze & Yang (2014), the dry deposited specimen tends to exhibit more contractive cyclic shear behaviour than the moist tamped one even under otherwise identical state and stress conditions. These results again support the notion that the α effect on K_σ is state-dependent.

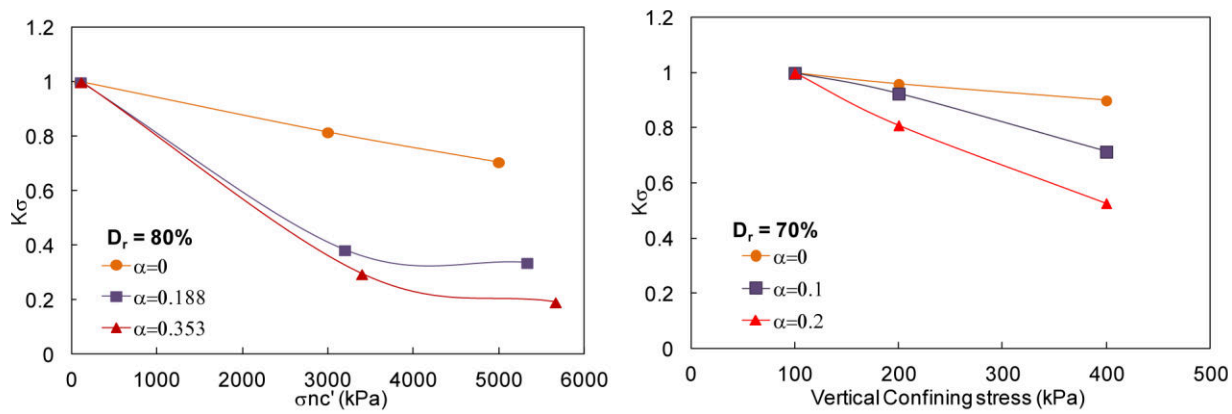

(a) (b)

Figure 7. Literature test results demonstrating the K_σ dependence on initial sustained shear stress (α) re-interpreted from: (a) Hyodo et al. (2002); (b) Sivathayalan & Ha (2004).

CONCLUSION

A review of the K_σ correction factor is presented in this paper. K_σ has been routinely adopted in geotechnical earthquake engineering design for extrapolating the cyclic liquefaction resistance of soil deduced from empirical correlation charts to account for the effects of higher overburden stress level. Its present form is a function of relative density of soil and overburden pressure only. Based on a comprehensive laboratory test database including a family of cyclic triaxial tests conducted by the authors and some relevant cyclic triaxial and simple shear tests obtained from the literature, it is found that K_σ is highly dependent on the level of shear stress initially sustained on the soil element. This so-called "α-effect" is state-dependent. The effect is more prominent in soil having a higher contractive state. Under the influence of a high sustained shear, K_σ drops substantially with increasing overburden pressure. This response cannot be captured by any of the present K_σ correlations rendering the current design potentially unconservative especially when initial static shear stress presents.

ACKNOWLEDGEMENTS

The tests reported and findings of the study were part of the post-graduate study of the first author. Financial support of this work was provided by the Research Grants Council of Hong Kong under Grant No. 719105 and 17250316. The work was also partially supported by the University of Hong Kong through the Research Output Prize Scheme. This paper is published with the permission of the Head of the Geotechnical Engineering Office and the Director of Civil Engineering and Development of the Government of the Hong Kong Special Administrative Region, China.

REFERENCES

Chan, C.K. (1981). "An Electropneumatic Cyclic Loading System." *Geot. Test. J.*, 4(4), 183-187.

Hyodo, M., Hyde, A.F.L., Aramaki N. and Nakata, Y. (2002). "Undrained Monotonic and Cyclic

Shear Behavior of Sand under Low and High Confining Stresses." *Soils & Found.*, 42(3), 63-76.

Idriss, I.M. and Boulanger, R.W. (2008). *Soil Liquefaction during Earthquakes.* Earthquake Engineering Research Institute, Oakland, CA.

Seed, H.B. (1983). "Earthquake-resistant Design of Earth Dams." *Proc., Symp. Seismic Design of Earth Dams & Caverns*, ASCE, New York, 41-64.

Seed, H.B. and Idriss, I.M. (1971). "Simplified Procedure for Evaluating Soil Liquefaction Potential." *J. Geot. Eng. Div.*, ASCE, 97(9), 1249-1273.

Sivathayalan, S. and Ha, D. (2004). "Effect of Initial Stress State on the Cyclic Simple Shear Behavior of Sands." in *Cyclic Behavior of Soils and Liquefaction Phenomena*, Triantafyllidis, ed., Taylor & Francis Group, London, 207-214.

Sze, H.Y. (2010). *Initial Shear and Confining Stress Effects on Cyclic Behaviour and Liquefaction Resistance of Sands*. PhD Thesis, The University of Hong Kong, 389 p.

Sze, H.Y. and Yang, J. (2014). "Failure Modes of Sand in Undrained Cyclic Loading: Impact of Sample Preparation." *J. Geot. & Geoen. Eng.*, ASCE, 140(1), 152-169.

Yang, J. and Sze, H.Y. (2010). "Failure of Saturated Sand in Non-symmetrical Cyclic Loading." *Proc, 5th Int. Conf. Recent Adv. in Geot. Earthq. Eng. & Soil Dyn.*, San Diego, U.S. Paper No. 1.25a.

Yang, J. and Sze, H.Y. (2011a). "Cyclic Behaviour and Resistance of Saturated Sand under Non-symmetrical Loading Conditions." *Géotechnique*, 61(1), 59-73.

Yang, J. and Sze, H.Y. (2011b). "Cyclic Strength of Sand under Sustained Shear Stress" *J. Geot. & Geoen. Eng.*, ASCE, 137(12), 1275-1285.

Youd, T.L., Idriss, I.M., Andrus, R.D., Castro, G., Christian, J.T., Dobry, R., Finn, W.D.L., Harder, L.F., Jr., Hynes, M.E., Ishihara, K., Koester, J.P., Liao, S.S.C., Marcuson III, W.F., Martin, G.R., Mitchell, J.K., Moriwaki, Y., Power, M.S., Robertson, P.K., Seed, R.B. and Stokoe II, K.H. (2001). "Liquefaction Resistance of Soils: Summary Report from the 1996 NCEER and 1998 NCEER/NSF Workshops on Evaluation of Liquefaction Resistance of Soils." *J. Geot. & Geoen. Eng.* ASCE, 127(10), 817-833.

Effectiveness of Stone Column in Liquefaction Mitigation

Sunita Kumari[1]; Vishwas A. Sawant[2]; and Siddharth Mehndiratta[3]

[1]Dept. of Civil Engineering, National Institute of Technology Patna, Patna 800005, India. E-mail: sunitafce@nitp.ac.in
[2]Dept. of Civil Engineering, Indian Institute of Technology Roorkee, Roorkee 247667, India. E-mail: sawntfce@iitr.ac.in
[3]Dept. of Civil Engineering, Indian Institute of Technology Roorkee, Roorkee 247667, India. E-mail: siddharth14feb@gmail.com

ABSTRACT

Failure of superstructure resting on shallow foundation is one of the most catastrophic phenomena occurring due to liquefaction during earthquake. The present paper presents the 3D numerical modelling of shallow foundation resting on liquefiable soil under earthquake loading. The benchmark model simulation has been simulated first to obtain the dynamic behavior of a loose sand deposit with a surface footing. The responses of this model treated with stone column improvement under the same seismic loading has been analyzed and compared with the response of benchmark models (BM), focusing on the evaluation of the strengthening effect of soil columns and its effect on the behavior of the remediated soil deposits. Acceleration base input excitation of El Centro earthquake is applied to each model to monitor the displacements, liquefaction potential, and excess pore pressures (EPP). Based on the response of the model, the relative effectiveness of stone columns as mitigation measure can be gauged. PLAXIS-3D finite element software is used for the analysis. A significant reduction in EPP and settlement are visible with the use of stone column as remedial measures.

INTRODUCTION

Liquefaction occurs frequently in saturated loose granular materials under earthquake and other dynamic loadings such as blasting. The structures resting on it, are most vulnerable to damage and destruction. During past earthquakes features like sand boiling, differential settlements, lateral spreading and loss of bearing strength beneath structures are seen due to liquefaction. Such type of failures have caused significant loss damaged life and built environment. Liquefaction mitigation measures include improvement of ground by removal and recompaction of low-density soils, removal of excess ground water, in situ ground densification, grouting, or surcharging. Use of stone column is a quite recent technique as compare to the traditional soil densification methods. If generation of high excess pore pressure takes place in the improved soil mass, the induced shear stresses during earthquake can be jointly distributed to dense gravel stone columns and the adjacent soil. This distribution is proportional to the relative stiffness of the composite materials, improving the overall stability of the system. Adalier et al. (2003) carried out centrifuge model tests on a silty sand (with and without a surcharge) treated with the application of stone column as remedial measures. The behavior of all these treated models was predicted and quantified with respect to the benchmark models under same cyclic loading conditions. Krishna et al. (2006) assessed liquefaction potential of soil with granular pile treatment. Seed and Booker's approach for pore pressure was modified to account for drainage and densification effect of granular pile (GP). Permeability and coefficient of volume compressibility of soil surrounding the soil were altered. Effect of GP on liquefaction behaviour was quantified in the detailed study. Krishna, (2011) presented an overview of the use of granular piles as a liquefaction remedial measure for sand deposits.

Presently, reliable numerical prediction of earthquake-induced liquefaction and settlements in foundation is still a great task (Arulanandan and Scott 1993, Parra 1996, Marcuson et al. 1996, Elgamal et al. 2003). The available computer programs for predicting seismically induced deformations are sophisticated and difficult to use (Finn, 2000). Full-scale testing and evaluation of remediated soil deposit under realistic earthquake conditions would be the most ideal method. However, it is highly expensive and in most cases too complex to put into practice. This paper describes the 3D numerical modelling of a loose sand stratum under earthquake loading. PLAXIS-3D finite element software is used for the analysis. Acceleration base input excitation of El Centro earthquake is applied to the models for monitoring the displacements, liquefaction potential and excess pore pressures (EPP). The benchmark model simulation was predicted first to obtain the dynamic behaviour of a loose sand deposit with surface footing. Then, the model was treated with stone columns for improvement. The response of this improved model subjected to the same seismic loading has been predicted and compared. The strengthening effect of stone columns and their effect on the behaviour of the remediated soil deposits have also been evaluated. Based on the response of the model, the relative effectiveness of stone columns as mitigation measure has been analysed. The capabilities and limitations of the employed numerical procedure for modelling such type of complicated phenomena are also considered.

PROBLEM STATEMENT

A soil domain of 13 m height, 22 m width and 13 m depth of loose sand having relative density (R_D) of 40% has been considered for the analysis in PLAXIS-3D. A surface foundation is applied to document the response of shallow foundation on liquefiable soil stratum. The El-Centro earthquake motion has been used as input ground motion. Response parameters in form of displacement resultants, liquefaction susceptibilities, excess pore pressures and other factors are studied. Identical model comprising stone column having relative density (R_D) of 90% as remedial measures has been also considered for numerical analysis. PLAXIS-3D uses the UBC3D-PLM model. This model is extended from UBCSAND model originally introduced by Peubla et al. (1997). The main characteristics of the model are briefly described by Shashank et al. (2015). The present analysis uses an effective stress analysis in which liquefaction occurs as a result of pore pressure generation. Undrained conditions are stimulated and volumetric strain and bulk modulus of water in pores is considered. Soil densification is also included to obtain higher accuracy in predicting EPP during seismic excitation. This mechanism permits for the increase of EPP with decreasing rates when shearing takes place. This behavior was also found in the experimental studies. In the dynamic analysis, it is required to absorb stresses at artificial boundaries to prevent reflection of waves. Viscous boundaries are considered at the boundary of the main domain which considers the Neumann type of boundary conditions, in which stresses at boundaries are updated to nullify the reflected stresses.

NUMERICAL INVESTIGATION

The first numerical analysis (Figure 1-a, Model 1) is performed for the benchmark model to explore the response of a 13 m thick loose sand stratum with surcharge applied through a rigid footing having relative density (R_D) of 40%. The surcharge of 144 kPa is designed to simulate the vertical pressure of a multistory reinforced concrete building. In the second analysis (Model 2), a total of 9 columns of 1.0 m diameter were placed with center-to-center spacing of 4 m in xdirection and 2.5 m in y-direction at preselected locations (Figure. 1-b.). The ground water table is assumed to be at the soil surface in all analysis. A 13 m thick horizontal soil layer is modelled with the borehole option in PLAXIS 3D. Stone columns are introduced in the structure mode. Soil and Stone columns are modeled using 10 node tetrahedral elements in continuation of soil, with different properties. It is assumed that the soil stratum is fully submerged in water. The numerical analysis is divided into different phases and specific types of analysis for each particular phase.

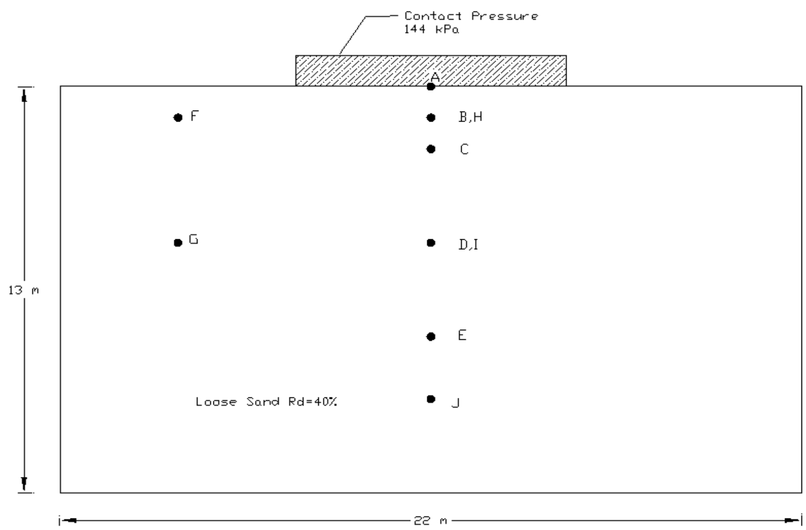

Figure 1-a. Benchmark model with footing (Model 1)

Table 1 Material properties and boundary conditions

Properties of loose sand stratum			
γ_{dry} =16.6 kN/m^3	γ_{sat} =16.64 kN/m^3	$e_{initial}$ = 0.667	E'=25 MPa
c' = 0 kPa	$k_x = k_y = k_z = 6.6\times10^{-5} m/s$	μ = 0.3	ϕ'=31°
Properties of stone column			
γ_{dry} =18.6 kN/m^3	γ_{sat} =20.4 kN/m^3	$e_{initial}$ = 0.546	E'=54 MPa
C' = 0 kPa	$k_x = k_y = k_z = 2.3\times10^{-5} m/s$	μ = 0.3	ϕ'=31°
Boundary conditions	X min :- Viscous X max:- Viscous	Y min:-Viscous Y max:- Viscous	Zmin:None Zmax:None

Material properties of the soil stratum and stone columns are reported in Table 1. Input model parameters for UBC3D-PLM are reported in Table 2. The correlation between normalised SPT values and relative density are taken from Cubrinovski et al., 1999. The SPT values are used as the input to find other values using formulae mentioned below. Permeability values and stone column properties were taken from Adalier et al., 2003. The input parameters are evaluated based on Brinkgreve et al. (2012):

$$\begin{aligned} \gamma_{unsat} &= 15 + 4.0\, R_D / 100 \quad (\text{kN/m}^3) \\ \gamma_{sat} &= 19 + 1.6\, R_D / 100 \quad (\text{kN/m}^3) \\ E_{oed}^{ref} &= 60000\, R_D / 100 \quad (\text{kN/m}^2) \end{aligned} \tag{1}$$

Galavi et al (2013) proposed equations for generic initial calibration as Follows:

$$\begin{aligned} K_G^e &= 21.7 \times 20 \times \left((N_1)_{60} \right)^{0.333} \quad ; \quad K_B^e = K_G^e \times 0.7 \\ K_G^p &= K_G^e \times \left((N_1)_{60} \right)^2 \times 0.003 + 100 \quad ; \quad R_f = 1.1 \times \left((N_1)_{60} \right)^{-0.15} \end{aligned} \tag{2}$$

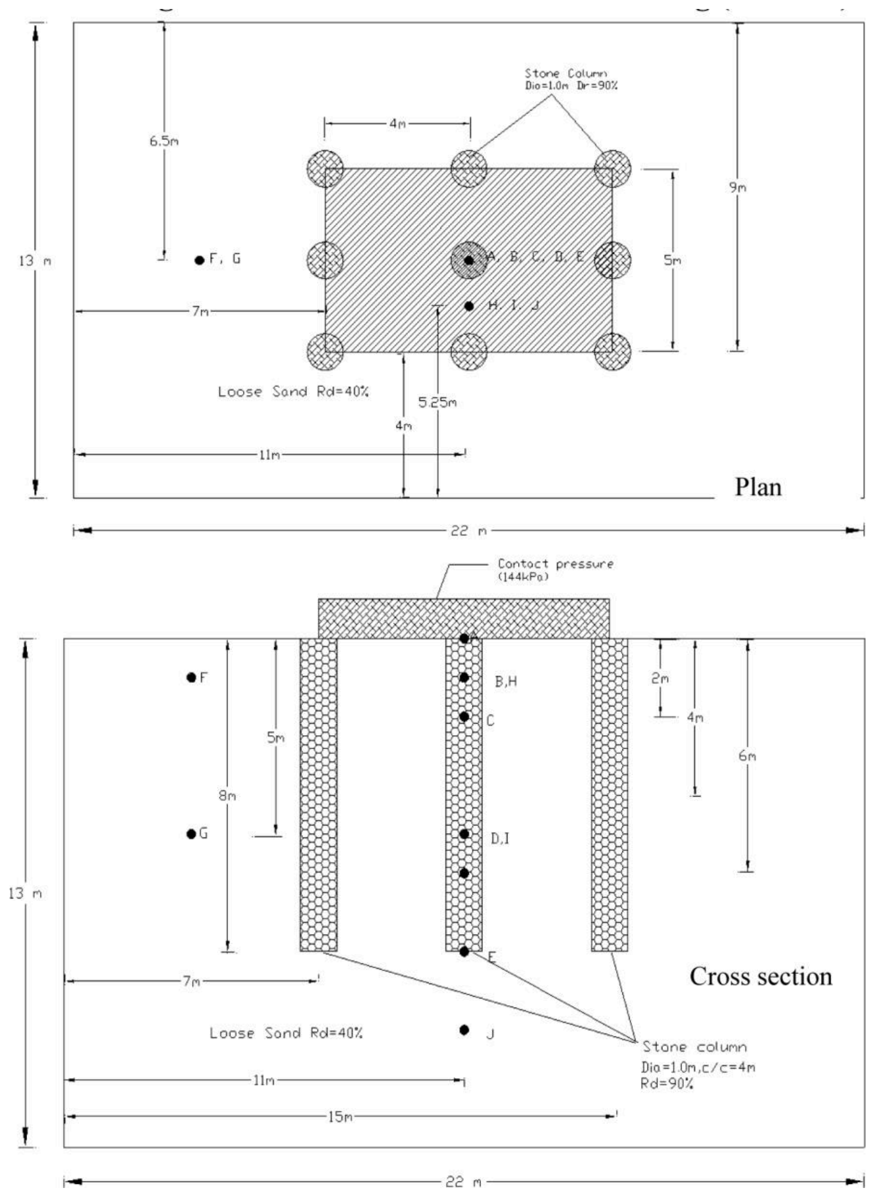

Figure 1-b. Benchmark model with Footing and stone Column (Model 2)

RESULTS AND DISCUSSION

Figure 2 shows the maximum value of displacement with respect depth at center of soil domain. A decrement of 45% in maximum displacement is observed in Model 2 as compared to Model 1 at top of soil domain. Figure 3 compares the computed vertical displacement with respect to time at different location of soil domain during the seismic event for Model 1 and Model 2. A maximum displacement of 99 cm and 54 cm are observed at location A (top most position of soil mass) for Model 1 and Model 2, respectively. These values are 47 cm and 24 cm at depth of 2 m (Location C). Similar trend are visible at other depth also for the above said models. A relatively less value of displacement is estimated away from the surcharge load (Location I). Predicted values for Model 2 are less than those evaluated for the benchmark Model 1 and the variation is noteworthy. Due to presence of a surcharge, stone columns are very effective in settlement reduction. A summary of maximum values of displacements is reported in Table 3. The displacements at A, D, F, I and others points are roughly uniform in nature with maximum values ranging from 1m to 12 cm which is decreasing with depth. The values obtained in Model 2 are about 50% less than those in Model 1, indicating the ability of the Model 2 to control the displacements produced during seismic shaking by showing stiffer composite-material behavior. Similar effect of stone column was reported in the centrifuge study by Adalier (2003).

Table 2 Input model parameters for UBC3D-PLM

Parameters with description	**Loose sand**	**Stone Column**
Peak friction angle (ϕ'_p)	33.65^0	40^0
Friction angle at constant volume (ϕ'_{cv})	33^0	37^0
Elastic shear modulus number (k_G^e)	809.4 kPa	890 kPa
Elastic bulk modulus number (k_B^e)	566.6 kPa	623 kPa
Plastic shear modulus number (k_G^p)	202.6 kPa	3755 kPa
Power for stress dependency elastic bulk modulus (n_k)	0.5	0.5
Power for stress dependency elastic shear modulus (n_g)	0.5	0.5
Power for stress dependency plastic shear modulus (n_p)	0.4	0.4
Failure ratio (R_f)	0.83	0.64
Reference stress (P_A)	100 kPa	100 kPa
Fitting parameter to adjust densification rule (f_{dens})	0.45	0.45
Fitting parameter for post liquefaction behavior (f_{post})	0.02	0.02
Corrected SPT blow counts $(N_1)_{60}$	6.5	37

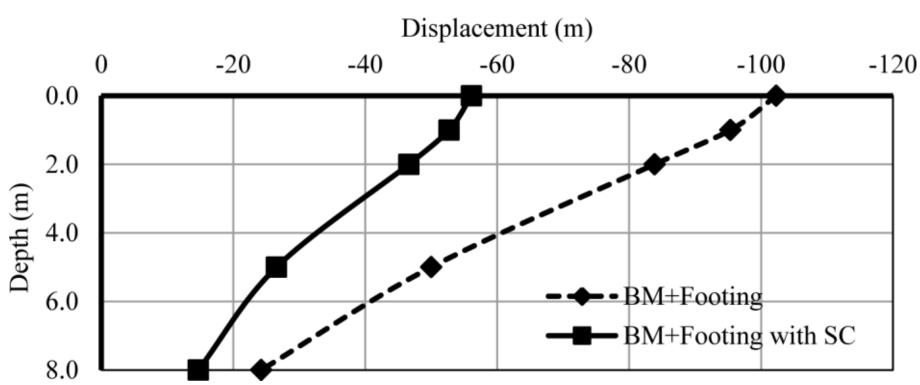

Figure 2. Comparison of displacement variation with depth

Table 3 Maximum Displacement of Bench Mark Model with Footing and BM with footing and sand column at different location

Location	BM with Footing				BM with Footing + SC			
	Ux (cm)	Uy (cm)	Uz (cm)	U	Ux (cm)	Uy (cm)	Uz (cm)	U
A	1.45	-0.79	-102.31	102.32	-13.87	-8.90	-56.12	58.49
B	1.90	-0.89	-95.37	95.39	-12.97	-9.97	-52.71	55.19
C	2.00	-0.40	-83.87	83.90	-12.58	-10.61	-46.61	49.43
D	1.72	-0.75	-50.01	50.04	-11.56	-15.86	-26.55	33.02
E	1.02	-0.92	-24.24	24.28	-11.66	-21.40	-14.71	28.46
F	1.90	-9.22	-89.64	90.13	-12.88	-16.97	-52.00	56.19
G	1.69	-7.26	-48.22	48.79	-11.23	-19.12	-24.85	33.31
H	0.48	-7.14	-9.87	12.19	-10.04	-28.01	-8.04	30.82
I	-6.18	0.27	-30.30	30.93	-15.65	-9.77	-12.00	22.01
J	-13.40	-0.58	-28.32	31.34	-22.33	-15.85	-15.10	31.27

The variations in EPP with respect to time at different locations in soil domain during the seismic loading for Model 1 and 2 are shown in figure 4. The computed EPP at different location (B, E, H and I) are compared with remedial measures (stone column). The maximum value of EPP at point B is 28.05 kPa without remedial measure whereas with stone column, it is reduced to 8.03 kPa. At point E (depth 8 m), a significant fall in EPP is observed in case of stone column. All EPP plots (Figure 4) show similar trend. After an initial rise, a peak is attained, and then the EPP remains more or less constant till the end of the earthquake. A significant reduction value of maximum EPP (104.81kPa) is visible in Model 2 as compared to maximum EPP (169.37 kPa) in Model 1. Similar trend is also reflected in the contours of normalized EPP (R_u) as described in figures 5 and 6. Comparisons of predicted accelerations for seismic excitation are shown in figures 7 and 8. In case of application of soil column, acceleration values have been reduced little as compared to the benchmark model. This is reflected in the reduced level of acceleration amplitudes. Similar trends are observed at different points of this model. A significant drop in magnitude of predicted acceleration is observed at all the locations after 30 seconds of loading.

CONCLUSIONS

This paper studies stone columns specifically to examine the effectiveness of remedial measures for liquefaction. The models with and without remedial countermeasures were analyzed. A comparative study was performed to highlight the effect of countermeasure on liquefaction. The stone column resulted in the smaller strains and cyclic mobility of the soil stratum. Maximum lateral strains and highest EPP in soil domain were observed in the no-remediation case with surcharge. Predicted values for the improved model (Model 2) are less than those observed for the unimproved model (i.e. Model 1) and the variation is noteworthy. Stone columns are very effective in settlement reduction. The values obtained in Model 2 are about 50% less than those in Model 1, signifying the competency of the Model 2 in controlling the displacement produced during seismic shaking showing stiffer composite-material behavior. A significant reduction value of maximum EPP (104.81kPa) is visible in Model 2 as compared to maximum EPP (169.37 kPa) in Model 1.

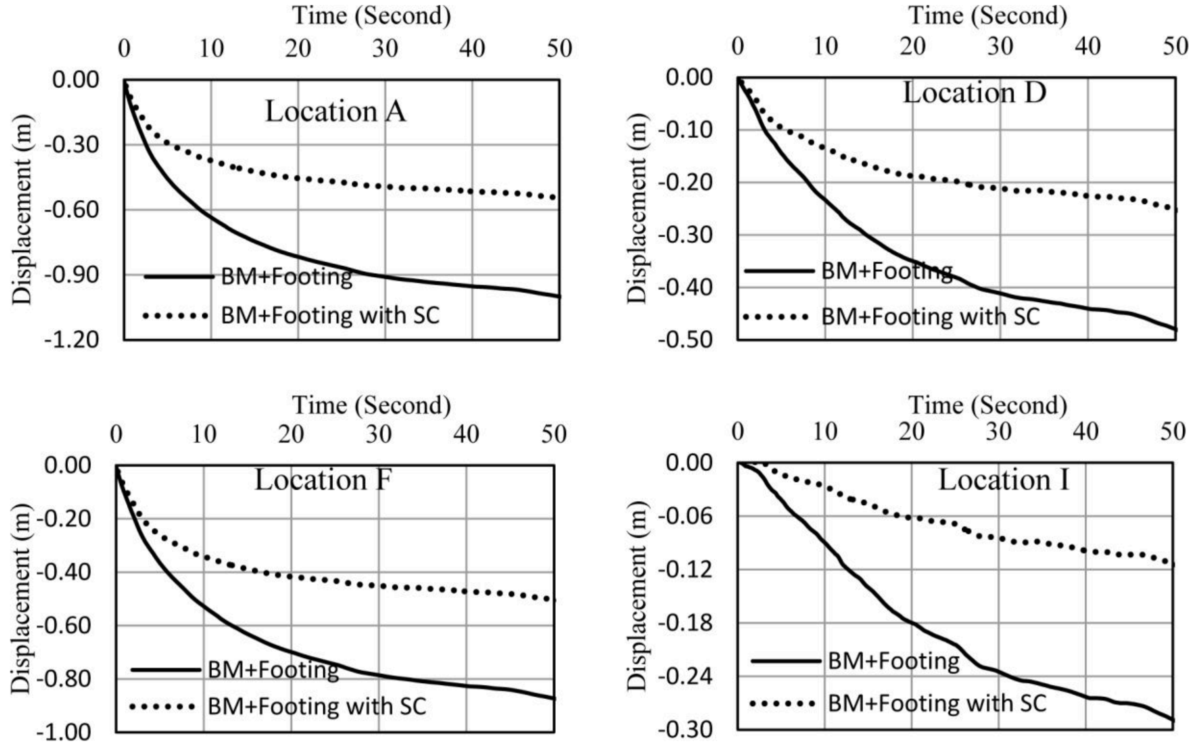

Figure 3. Comparison of displacement variation with time at different location

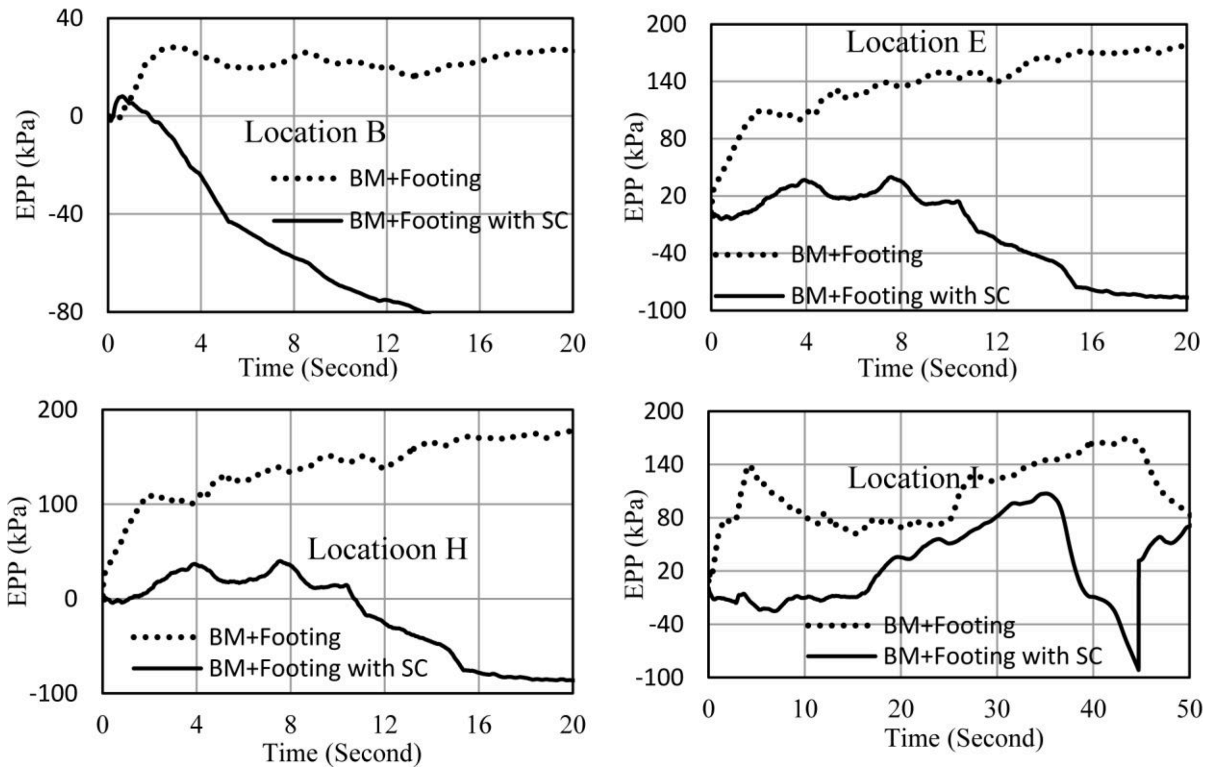

Figure 4. Comparison of EPP variation with time at different location

The results of this study show that numerical modeling of earthquake effects on liquefiable soil strata with and without remedial measures is feasible using the common laboratory test